OneDimensional Model of a Lorentz Plasma

Ramy Shanny, John M. Dawson, and John M. Greene

Citation: Physics of Fluids (1958-1988) **10**, 1281 (1967); doi: 10.1063/1.1762273
View online: http://dx.doi.org/10.1063/1.1762273
View Table of Contents: http://scitation.aip.org/content/aip/journal/pof1/10/6?ver=pdfcov
Published by the AIP Publishing

One-Dimensional Model of a Lorentz Plasma

RAMY SHANNY,* JOHN M. DAWSON, AND JOHN M. GREENE
Plasma Physics Laboratory, Princeton University, Princeton, New Jersey
(Received 3 January 1967)

A one-dimensional electron plasma model, in which electron sheets can scatter in three dimensions in velocity space through small-angle collisions with the stationary ions, has been constructed. Using the model, the dc conductivity of a Lorentz plasma is measured. The result agrees with the theoretical prediction, therefore confirming the validity of the model and exhibiting its capability for determining other transport coefficients. The decay rate of a standing wave when collisions are present is measured. The result verifies the theoretical result, in which the various decay increments are superimposed. The wavelength dependence of the collisional damping is observed.

I. INTRODUCTION

RESEARCH in plasma physics, as in most other fields of science, is accomplished through experiments and theoretical work. However, due to the intricate nature of a laboratory plasma, the comparison between experimental and theoretical work has not always been possible. In order to alleviate some of the difficulty a scheme can be devised by which one follows the exact dynamics of particles numerically on a high-speed digital computer. Such a method can be called computer experiments.

This approach to predicting physical phenomena and verifying analytical work has been fruitfully employed by a number of workers in plasma physics.[1-10] A one-dimensional plasma model is described in Ref. 1. The relevance of the model is discussed, and numerical experiments connected with the behavior of a plasma at thermal equilibrium are described there. The results of the experiment are in agreement with the theoretical predictions. This model has also been used to follow the evolution of a double-stream instability,[2] and the thermalization of a square-shaped velocity distribution.[3] A similar model representing a two-species plasma, was constructed by Smith and Dawson.[4] Drift instabilities, two-stream instability, and ion waves were studied numerically with that model. Eldridge and Feix[5] have used a similar two-species model for thermal equilibrium studies. Numerical experiments describing the breaking up of large-amplitude waves in a cold plasma were performed by Buneman.[6,7] A model representing a two-species plasma including a magnetic field was constructed by Auer, Hurwitz and Kilb.[8] Using the model, shock waves were studied. Their model involved fluid-like approximations beyond the calculation of particle trajectories. Another model describing a two-species plasma in a magnetic field, following coarse-grained particle trajectories, was constructed by Hockney.[9] Using that model, flute instabilities were studied successfully.

Except for collisions, the model used here is the same as discussed in Ref. 1. The model represents a plasma with no magnetic field and a one-dimensional electric field. Electrons are represented by infinite sheets having three velocity coordinates and one position coordinate. Ions are infinitely heavy, stationary, and uniformly distributed through the plasma (smeared ion background). An electron sheet can interact with other electrons and with the smeared-out ion background through the one-dimensional electric field. Collisions with ions are included through a random scattering of the sheet velocities. The model follows the trajectory of each sheet. Therefore the numerical solutions obtained by the model are identical to solutions of the Liouville equation for a finite number of particles, with the same geometrical restrictions.

Once the model is constructed and programmed for numerical computations, it can be viewed as an experimental machine equipped with exact measuring devices. The number of possible experiments using this device is very large. The work presented here has by no means exhausted the usefulness of the model. The results of two experiments are presented here. The first one is the measurement of the dc conductivity. The purpose of this experiment

* Present address: General Electric Space Science Laboratory, King of Prussia, Pennsylvania.

1 J. M. Dawson, Phys. Fluids 5, 445 (1962).
2 J. M. Dawson, Nucl. Fusion Suppl. Pt. 3, 1033 (1962).
3 J. M. Dawson, Phys. Fluids 7, 419 (1964).
4 C. Smith and J. M. Dawson, Princeton Plasma Physics Laboratory Report MATT-151, (1963).
5 O. C. Eldridge and M. Feix, Phys. Fluids 5, 1076 (1962).
6 O. Buneman, Phys. Rev. 115, 503 (1959).
7 O. Buneman, J. Nucl. Energy, Pt. C2, 119 (1961).
8 P. L. Auer, H. Hurwitz, Jr., and R. W. Kilb, Phys. Fluids 4, 1105 (1961).
9 R. W. Hockney, Phys. Fluids 9, 1826 (1966).
10 A. Hasegawa and C. K. Birdsall, Phys. Fluids 7, 1590 (1964).

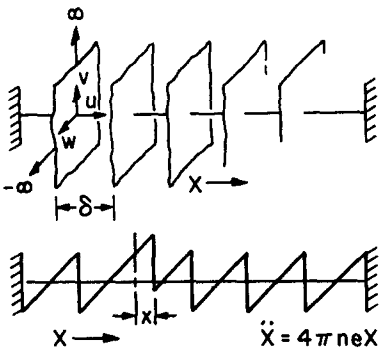

FIG. 1. One-dimensional plasma model, illustrating the electron sheets and the electric field.

is to establish the validity of the model and show that it can be used to determine transport coefficients. The results agree with the theory within the statistical error involved (15%). A more exact result could be obtained by continuing the computation for a longer time. However, the problem does not merit the added cost involved. The second experiment examines the decay of a small-amplitude wave when ion–electron collisions are present. The results are in good agreement with the theory.[11] The experiment serves as an illustration of the usefulness of the model in confirming analytical work.

II. MODEL

The model presented here simulates a one-dimensional electron plasma in which electrons can scatter in three dimensions in velocity space through small-angle collisions with the stationary ions. The one-dimensional plasma model was constructed and fully described in Ref. 1. We assume familiarity of the reader with that model and describe in detail only the novel features used here. These are the treatment of the three-dimensional velocity space, the transformation to a moving frame, boundary conditions, the method of including collisions, and the initial conditions.

The electrons are represented by infinite sheets embedded in a uniform background of infinitely heavy ions. The motion of the electron sheets is specified by three velocity coordinates, U_x, U_y, and U_z, and one-space coordinate, X, see Fig. 1. As the sheets are infinite, the system is invariant to displacements in the transverse directions. Thus the motion is independent of the y and z coordinates. We will assume rotational symmetry of the transverse velocities around the x axis, so the motion can be described by a velocity component in the longitudinal direction, U, and a transverse velocity, v, where v is always positive. The transverse motion acts as an energy reservoir for the longitudinal motion, and the fixed ions act as a momentum reservoir. There is no exchange of energy between the electrons and ions, and the only energy exchange between the transverse and longitudinal motions is through the scattering by the ions.

[11] G. G. Comisar, Phys. Fluids 6, 76 (1963).

The equation of motion of a single sheet, in the absence of crossing as discussed in Ref. 1 and in the absence of collisions with the ions, is given by

$$\ddot{X}_i + \omega_p^2(X_i - X_{0i}) = 0. \tag{1}$$

Here X_i is the position of the sheet measured in the frame in which the computations are made and which we call the lab frame. This is also the frame in which the ions are held fixed. The quantity ω_p is the plasma frequency, and X_{0i} is the equilibrium position of the sheet. The electron sheets can only oscillate about their equilibrium positions and exchange these positions with other electron sheets. Thus, if the equilibrium positions are held fixed, the mean electron velocity must vanish. In order to have a nonvanishing mean electron velocity the quantities X_{0i} must increase linearly with time:

$$X_{0i} = C(t + t_{0i}). \tag{2}$$

The quantity C is the mean electron velocity, and the parameters t_{0i} allow the initial values of the equilibrium positions to be prescribed.

The solution of Eq. (1), giving X, $\dot{X}$, and X_0 at a time $t + \Delta t$ in terms of the known values of these quantities at a time t, is

$$X_i(t + \Delta t) = [X_i(t) - X_{0i}(t)] \cos \omega_p \Delta t + \frac{1}{\omega_p} [\dot{X}_i(t) - C] \sin \omega_p \Delta t + C \Delta t + X_{0i}(t), \tag{3}$$

$$\dot{X}_i(t + \Delta t) = [\dot{X}_i(t) - C] \cos \omega_p \Delta t - \omega_p[X_i(t) - X_{0i}(t)] \sin \omega_p \Delta t + C, \tag{4}$$

$$X_{0i}(t + \Delta t) = C \Delta t + X_{0i}(t). \tag{5}$$

These equations, plus the corrections for crossing of the sheets, are used to advance the model in time. The time-steps are taken sufficiently small that the crossing corrections can be simply and accurately approximated.

Two general types of boundary conditions can be used; reflecting boundary conditions and periodic boundary conditions. In Ref. 1 the plasma was bounded by perfectly reflecting walls which simply changed the sign of the velocity of the particles. The normal modes of oscillation of such a system must be standing waves. When periodic boundary conditions are used, an electron sheet which leaves the considered region reappears on the other side with the same velocity. With these boundary conditions, the plasma can support traveling waves. Both types of boundary conditions were used in the results quoted in this paper.

Collisions between the sheets and background ions are taken into account at the end of each time step in the following manner. It is postulated that during a time step Δt a number of small-angle collisions have taken place, each with a different orbit plane. As a result of these collisions the magnitude of the velocity is unchanged, but its direction is altered. The two quantities which describe this deflection are the angle of deflection, which we denote by ϕ, and the angle this deflection makes with the U, v plane, denoted by ψ (see Fig. 2). The angle ψ is chosen randomly with a uniform distribution between 0 and 2π. The distribution of ϕ is taken to agree with the Spitzer formula for small-angle scattering. The differential probability for a scattering lying in the range between ϕ and $\phi + d\phi$ is

$$P(\phi)\, d\phi = (\phi\, d\phi/\langle\phi^2\rangle\, \Delta t) \exp\,[-\phi^2/(2\langle\phi^2\rangle\, \Delta t)], \quad (6)$$

where

$$\langle\phi^2\rangle = (3\omega_p/2\Lambda) \ln \Lambda \quad (7)$$

$$\Lambda = 6\pi(n/Z)[U^2 + v^2)/\omega_p^2]^{\frac{3}{2}}, \quad (8)$$

and Z/n is a constant that can be chosen for convenience.

The most common series of random numbers are uniformly distributed between 0 and 1. In order to use such a series to generate the scattering distribution we proceed as follows. Let $\alpha(\phi)$ be such a function of ϕ that α takes on values from 0 to 1 when ϕ runs over its range of values. Let the probability density of finding α in $d\alpha$ be unity, i.e., the values of α are uniformly distributed between 0 and 1. We then have

$$P(\alpha)\, d\alpha = d\alpha = (d\alpha/d\phi)\, d\phi = P(\phi)\, d\phi. \quad (9)$$

Taking α equal to zero when ϕ equals zero we have

$$\alpha(\phi) = \int_0^\phi P(\phi)\, d\phi. \quad (10)$$

We take r to be a random number with uniform distribution between 0 and 1. We then determine ϕ by

$$\phi = \alpha^{-1}(r); \quad (11)$$

ϕ has the desired distribution. In the present case

$$\alpha(\phi) = 1 - \exp\,[-\phi^2/(2\langle\phi^2\rangle\, \Delta t)], \quad (12)$$

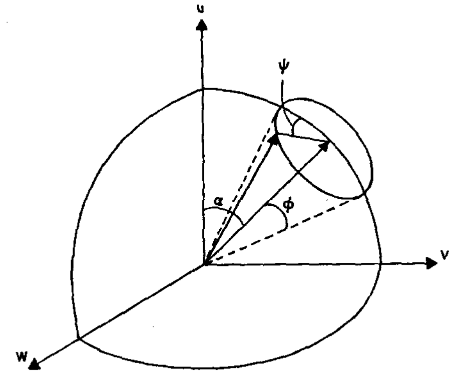

FIG. 2. Scattering of the velocity vector. The quantity α is the initial inclination of the velocity vector to the x axis, ϕ is the magnitude of the scattering, and ψ is the orientation of the scattering relative to the x axis.

so that

$$\phi = [-2\langle\phi^2\rangle\, \Delta t \ln\,(1 - r)]^{\frac{1}{2}}. \quad (13)$$

It is shown in the Appendix that this collision term, cumulated over many increments in time and in the limit as Δt becomes small, simulates a Lorentz gas collision term of the form:

$$\frac{\partial}{\partial t} P(V, \theta, t) = \nu(V) \frac{1}{\sin\,\theta} \frac{\partial}{\partial \theta} \sin\,\theta \frac{\partial}{\partial \theta} P(V, \theta, t), \quad (14)$$

where $U = V \cos\,\theta$, $v = V \sin\,\theta$, and the collision frequency ν,

$$\nu = \tfrac{1}{2}\langle\phi^2\rangle, \quad (15)$$

is velocity-dependent.

Initially all electron sheets are placed at their equilibrium positions and the equilibrium positions are equidistant. The transverse velocities are given a Maxwellian distribution,

$$f(v)\, dv = (v/\langle v^2\rangle) \exp\,(-v^2/2\langle v^2\rangle)\, dv. \quad (16)$$

This was generated by computing the integral probability, exactly as shown above for the collisional scattering.

The initial longitudinal velocities are computed as the sum of several components. The random component with a Gaussian distribution gives the thermal energy. A Gaussian distribution can be formed by computing the integral probability, following the scheme outlined above, but this involves inverting the error function. An alternate method, which was used, is to add a series of random numbers which are uniformly distributed between 0 and 1. In the limit as the number of terms, N, becomes large, the sum has a Gaussian distribution centered at $\frac{1}{2}N$ and with standard deviation $N^{\frac{1}{2}}$. This distribution can be shifted and stretched to fit the desired values.

The second component consists of initial correlations of the velocity with position and is introduced to produce waves.

According to kinetic theory, and in actual practice, the initial correlation of the sheets decays rapidly. After a few plasma oscillation times the spatial correlation has the expected value for the longitudinal velocity distribution, and, at the same time, any small deviations from a Maxwellian are rapidly washed out.

III. RESULTS

The number of experiments possible with the model is very large. In this paper, only two experiments are presented. These have been selected to illustrate the usefulness of the model.

A. Direct Current Conductivity

The theory predicting the dc conductivity of a Lorentz plasma in the absence of a magnetic field is well established. The purpose of the numerical experiment is to verify the validity of the collision aspect of the model. Once the validity of the model is established, it can be used with confidence in other problems.

A constant current was generated by fixing C in Eq. (2), the velocity of the equilibrium positions. Then the voltage drop across the plasma was measured. This can be done as follows. The electric field at a point $X = \xi$ between the sheet labeled i–1 and that labeled i is

$$(e/m)E = \omega_p^2[\xi - \tfrac{1}{2}X_{0i-1} - \tfrac{1}{2}X_{0i}]. \qquad (17)$$

The voltage difference between these sheets is

$$\begin{aligned}\frac{e}{m}\,\Delta V &= \int_{X_{i-1}}^{X_i} \frac{e}{m}\,E\,d\xi \\ &= \tfrac{1}{2}\omega_p^2[(X_i - X_{0i})^2 - (X_{i-1} - X_{0i-1})^2 \\ &\quad + (X_{0i} - X_{0i-1})(X_i - X_{0i} + X_{i-1} - X_{0i-1})]. \qquad (18)\end{aligned}$$

Summing over all sheets and using periodic boundary conditions, we find the total voltage drop across the plasma is simply

$$\frac{e}{m}\,V = \omega_p^2\,\delta \sum_i (X_i - X_{0i}), \qquad (19)$$

where δ is the separation of equilibrium positions. This quantity clearly measures the drag on the electrons as the equilibrium positions are pulled through the ions. The resistivity is simply calculated as the ratio of the voltage to the current.

One difficulty that is encountered is that the energy dissipation continuously increases the temperature of the plasma and thus affects the resistivity. To obtain longer averages at constant temperature it was found desirable to extract energy from the plasma. This was done by periodically reducing the energy of each particle by a constant factor (independent of v), adjusted according to the energy dissipation in the interval.

A more vexing problem was the presence of noise in the measured voltage. The system has a strong resonance at the plasma frequency. Because this oscillation is weakly damped, it is coherent over long periods of time, times of the order of a collision time, and the thermal level of fluctuation is annoyingly large. We allowed one collision time for the system to come to equilibrium, and then used the coherence of the noise to fit the measured voltage to

$$V = V_0 + V_c \cos\omega_p t + V_s \sin\omega_p t. \qquad (20)$$

The constant term is then the dc value to be used in determining the conductivity. The values of V_c and V_s are not constant, becoming incoherent with the initial state, after a collision time as would be expected.

The above procedure is identical to a time average of the voltage as defined by Eq. (21):

$$\frac{e}{m}\,V_0 = \omega_p^2\,\frac{\delta}{\Delta T}\int_T^{T+\Delta T} \sum_i (X_i - X_{0i})\,dt; \qquad (21)$$

similarly, the mean current is given by

$$\frac{e}{m}\,j = \frac{\omega_p^2}{4\pi N\,\Delta T}\int_T^{T+\Delta T} \sum_{i=1}^{N} \dot{X}_i\,dt. \qquad (22)$$

The resistivity is defined by the ratio of the electric field to the current, as given by Eq. (23)

$$\eta = 4\pi \int_T^{T+\Delta T} \sum_i (X_i - X_{i0})\,dt \bigg/ \int_T^{T+\Delta T} \sum_i \dot{X}_i\,dt. \qquad (23)$$

The resistivity is given theoretically[12] as

$$\eta_L = (\tfrac{1}{2}\pi)^{\frac{3}{2}}(2\omega_p^2)^{-1}\langle\phi^2\rangle_t, \qquad (24)$$

where $\langle\phi^2\rangle_t$ is defined by Eq. (7) and evaluated at $U^2 + v^2 = kT/m$. The theoretical value of the resistivity using the experimental input parameters is $0.392\omega_p^{-1}$, while the experimental value is $0.435\omega_p^{-1}$. The difference is 11.5% which is within the statistical error of ±15% for this particular experiment. This lends confidence to further use of the model for examining problems in which electron–ion collisions are important. A plot of the electric field and current versus time is given in Fig. 3.

[12] L. Spitzer, Jr., *Physics of Fully Ionized Gases* (Interscience Publishers, Inc., New York, 1962), 2nd ed.

The theoretical value for the conductivity is accurate roughly to $(\ln \Lambda)^{-1}$ which is 10%. The accuracy of the numerical experiment was not sufficient to catch effects of this size. With longer runs more accurate results could have been obtained. However, any such deviations for the model would be spurious since it does not include effects such as large-angle scattering which are also of this order. We did not feel the problem merited the added expense.

B. Effect of Ion–Electron Collisions on the Decay of a Landau Damping Wave

The purpose of this work is to verify the theoretical work on the effect of electron–ion collisions on the decay of a Landau-damped wave.[11] The problem is simulated by the model, and solved numerically in the following manner. First, at $t = 0$, all the sheets are placed in their equilibrium position, and given such velocities that their velocity distribution is Maxwellian with a specified temperature, yielding a Debye length $\lambda_D \equiv \omega_p^{-1}(kT/m)^{\frac{1}{2}}$ of 16 δ, where δ is the intersheet spacing. The number of sheets in the system is 1000. Then a standing wave is superimposed by adding the velocity,

$$U_i = \sqrt{2}\, \epsilon \lambda_D \omega_p \sin [K\, \delta i], \tag{25}$$

to the velocity of the ith sheet. The quantity ϵ is a nondimensional amplitude, chosen in this case to equal 0.1, and K is the wavenumber, chosen equal to $6\pi/1000\ \delta$.

The theoretical Landau damping rate, γ_L, for such a wave is given by

$$\gamma_L = \frac{\pi\omega}{2} \frac{K}{\omega} \frac{d\omega}{dK} \frac{\omega_p^2}{K^2} \frac{\partial f}{\partial v}\bigg|_{\omega/K}. \tag{26}$$

Using the experimental parameters, $\gamma_L = 0.0332\omega_p$.

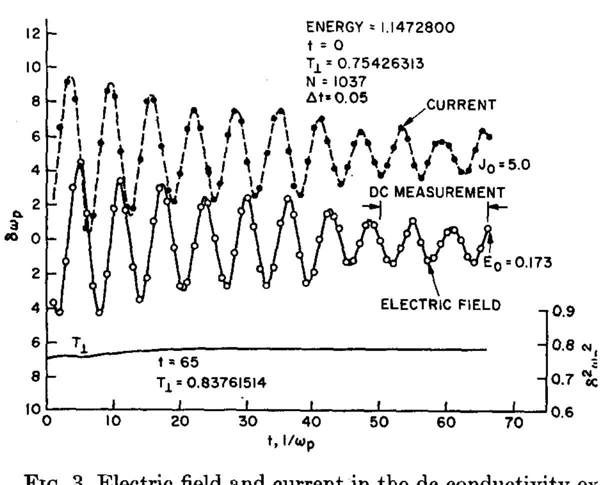

FIG. 3. Electric field and current in the dc conductivity experiment. The upper curve gives $4\pi ej/m\omega_p^2$ in units of $\delta\omega_p$, the next curve gives the average electric field $eV_0/mN\delta$ in units of $\omega_p^2\delta$, the lower curve gives the temperature.

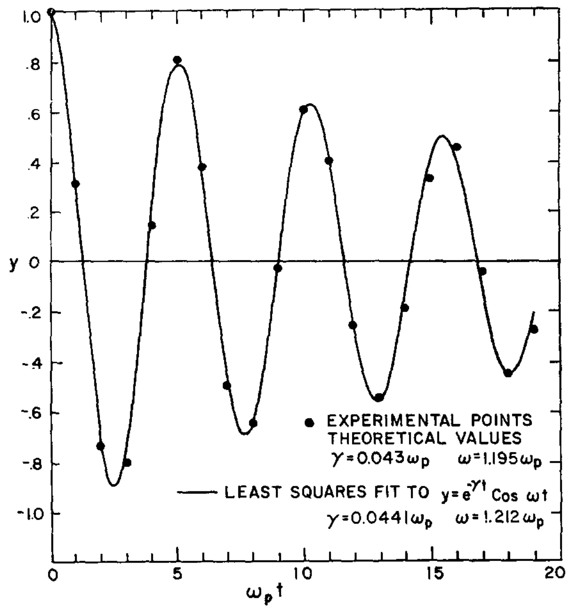

FIG. 4. Decay of a wave by Landau damping and ion–electron collisions.

The theoretical damping rate is based on the results of work done by Comisar[11] in which a Fokker–Planck equation incorporating ion–electron and electron–electron collisions was solved. The decay of the electric field is described by superposition of the three decay mechanisms: Landau damping, and the two collisional effects, ion–electron and electron–electron. The decay of the electric field E_K, in the absence of electron–electron collisions which are absent in this model, is given by

$$\partial E_K/\partial t = -E_K(\gamma_L + \gamma_{\mathrm{coll}}), \tag{27}$$

where γ_{coll} is given by

$$\gamma_{\mathrm{coll}} = \frac{\nu_t}{3(2\pi)^{\frac{1}{2}}} [1 + 4(K\lambda_D)^2], \tag{28}$$

and ν_t is the collision frequency defined by Eq. (15) evaluated at $U^2 + v^2 = kT/m$. For the parameters in this experiment $\gamma_{\mathrm{coll}} = 0.0097\omega_p$, $\nu_t = 0.053\omega_p$. The $k\lambda_D$ term contributes 54% of γ_{coll}, or 8% of the total damping. The over-all decay rate is $0.043\omega_p$ and the frequency is $1.195\omega_p$.

Comparison between these theoretical results and the experiment are shown in Fig. 4. The experimental points are three-run averages of the correlation function, $y(t)$, normalized to unity for t equal zero,

$$y(t) = \frac{N(0)}{N(t)} \frac{\sum_i E_K(t_i)E_K(t_i + t)}{\sum_i E_K^2(t_i)}, \tag{29}$$

$$t_i = n\omega_p^{-1}, \quad n \text{ an integer.}$$

Here $N(0)$ and $N(t)$ are the number of terms in the sums for time delays 0 and t; there were roughly a total of 50 sampling times per run. The wave of interest had an initial amplitude 3.15 times the thermal level and an energy of 10 times its thermal energy.

In an experiment of this type, a certain experimental error results from the random motion of the particles and from the random collisions. The motion of the amplitude is like the Brownian motion of an oscillator. The spread in amplitudes for many runs goes like[13] $A_T(1 - e^{-2t/t_D})^{\frac{1}{2}}$ where t_D is the damping time and A_t is the thermal amplitude. For the case run, the damping time was $22.2\omega_p^{-1}$ while the last experimental point is at $\omega_p t = 19$. Thus for one run and no time averaging as is given by (29), we would expect a deviation of $0.9A_T$ from the mean amplitude for many runs. The percentage error in the damping would be roughly $0.9A_T/2A_T \approx 45\%$. This error is reduced by a factor of $3^{-\frac{1}{2}}$ by averaging over 3 runs. The error reduction due to the time averaging used in (29) can be estimated from the theory of Brownian motion. This theory indicates that roughly each time sample can be considered independent. However, the mean initial amplitude decreases from $3A_T$ for t_i equals zero to $1A_T$ for $t_i = 30$. A mean starting amplitude of $2A_T$ seems like a reasonable estimate. The sum should thus reduce the error by the factor $(2 \times 30/3)^{-\frac{1}{2}}$. The total error reduction should be roughly a factor of 8. This gives an expected error in the damping coefficient of $5 \sim 6\%$.

The experimental points were fitted to a curve of the form

$$y(t) = e^{-\gamma t} \cos \omega t \tag{30}$$

by means of least squares. When half and two-thirds of the points were used to obtain γ and ω, these values deviated from those obtained by using all the points by 6% and 2%, respectively. This indicates that the uncertainty in the fit is of the order of 5% which is in good agreement with our estimate.

The least-squares values of γ and ω deviate by only 2% from the theoretical values. However, the actual accuracy is probably nearer the 5% we estimated. This error is less than the 8% correction to the damping due to the finite wavelength as given by (28). Thus it appears that we have verified the need for this term and that its magnitude is correct to better than a factor of 2.

This experiment shows that the superposition of decay rates holds for these conditions. The superposition of decay rates is not obvious to the physical intuition, as one may suppose that collisions may destroy the coherent acceleration and deceleration of electrons at the phase velocity and therefore affect the Landau damping rate.

It should be remarked that the same experiment was performed with ion–electron collisions turned off. The results were in excellent agreement with theory.

Results of an experiment in which the excited wave was of nonlinear amplitude indicate that ion–electron collisions have very small effect for a reasonable choice of collision frequency. This result will be presented in conjunction with nonlinear studies.

IV. CONCLUSION

A model has been constructed suitable for simulating a Lorentz plasma numerically using a high-speed digital computer. The results obtained describe the behavior of an electron plasma where the electrons undergo collisions with stationary ions. The model can be used for verifying theories and predicting the behavior of a plasma for some given initial and boundary conditions. The validity of the analytical work by Comisar,[11] in which the damping can be represented by a superposition of collisional and Landau damping, is confirmed. The predicted dependence of the collisional damping on the wavelength is observed.

ACKNOWLEDGMENTS

We wish to thank the Plasma Physics Laboratory Computing Group, and especially A. Stutz, for their advice and assistance.

This work was performed under the auspices of the United States Atomic Energy Commission, Contract No. AT(30-1)-1238. Use was made of computer facilities supported in part by National Science Foundation Grant NSF-GP579.

APPENDIX A: DERIVATION OF THE FOKKER–PLANCK EQUATION

In this section we demonstrate that the ion–electron collision routine is identical to the Fokker–Planck collision term.

Consider a velocity vector of fixed magnitude in a three-dimensional space. The locus of a small deflection of the velocity vector is a cone with an

[13] S. Chandrasekhar, G. E. Uhlenbeck, and L. S. Ornstein, M. C. Wang and G. E. Uhlenbeck, S. O. Rice, M. Kac, and J. L. Doob, in *Selected Papers on Noise and Stochastic Processes*, Nelson Wax, Ed. (Dover Publications, Inc., New York, 1954).

angle 2ϕ. Since the space is invariant to rotation, for simplicity we will place the cone axis to coincide with the z axis. The velocity vector after collision is described by

$$V_x = V \sin\phi \cos\psi,\quad V_y = V \sin\phi \sin\psi,\quad V_z = V \cos\phi. \tag{A1}$$

The probability of having an angle less than ϕ, and less than ψ, after a time increment Δt, is specified in the collision routine, and is defined by

$$P_1(\phi, \psi) = \tilde{P}_1(\phi)\, \tilde{\tilde{P}}_1(\psi), \tag{A2}$$

where

$$\tilde{P}_1(\phi) = \frac{1}{\langle\phi^2\rangle\, \Delta t} \int_0^\phi \phi' \exp\left[-\frac{\phi'^2}{2\langle\phi^2\rangle\, \Delta t}\right] d\phi', \tag{A3}$$

$$\tilde{\tilde{P}}_1(\psi) = \frac{1}{2\pi} \int_0^\psi d\psi'. \tag{A4}$$

We now desire to describe the behavior of the probability of having a certain velocity vector at time t. This is done by the following standard method.

$$\begin{aligned} P(\mathbf{V}, t) &= \iint P(\mathbf{V} - \Delta\mathbf{V}, t - \Delta t) P_1(\phi, \psi)\, d\phi\, d\psi \\ &= \iint \left[P(\mathbf{V}, t - \Delta t) - \Delta\mathbf{V}\cdot\frac{\partial P}{\partial \mathbf{V}} + (\Delta\mathbf{V}\,\Delta\mathbf{V}) : \frac{\partial^2 P}{\partial\mathbf{V}\,\partial\mathbf{V}} + \cdots\right] \\ &\quad \cdot P_1(\phi, \psi)\, d\phi\, d\psi. \end{aligned} \tag{A5}$$

Dividing Eq. (A5) by Δt, taking the limit of $\Delta t \to 0$, and performing the integration, we get

$$\frac{\partial P}{\partial t} = \lim_{\Delta t \to 0} \sum_{i=1}^{3} \left(-\frac{\langle\Delta v_i\rangle}{\Delta t} \frac{\partial P}{\partial v_i} + \sum_{j=1}^{3} \frac{\langle\Delta v_i\, \Delta v_j\rangle}{\Delta t} \frac{\partial^2 P}{\partial v_i\, \partial v_j} + \cdots\right). \tag{A6}$$

Equation (A6) is a complete solution; however, it is useless unless the coefficients are evaluated using the specified probability functions. Using Eqs. (A1), (A3), and (A4) we can evaluate the coefficients,

$$\frac{\langle\Delta v_i\rangle}{\Delta t} = \frac{1}{\Delta t} \iint \Delta v_i\, \tilde{P}_1(\phi) \tilde{\tilde{P}}_1(\psi)\, d\phi\, d\psi, \tag{A7}$$

$$\frac{\langle\Delta v_i\, \Delta v_j\rangle}{\Delta t} = \frac{1}{\Delta t} \iint \Delta v_i\, \Delta v_j\, \tilde{P}_1(\phi) \tilde{\tilde{P}}_1(\psi)\, d\phi\, d\psi. \tag{A8}$$

The results of Eqs. (A7) and (A8) are

$$\langle\Delta v_x\rangle/\Delta t = \langle\Delta v_y\rangle/\Delta t = \langle\Delta v_z\rangle/\Delta t = 0, \tag{A9}$$

$$\begin{aligned} \langle\Delta v_x\, \Delta v_y\rangle/\Delta t &= \langle\Delta v_x\, \Delta v_z\rangle/\Delta t \\ &= \langle\Delta v_y\, \Delta v_z\rangle/\Delta t = 0, \end{aligned} \tag{A10}$$

$$\begin{aligned} \langle\Delta v_x^2\rangle/\Delta t &= \tfrac{1}{2}\langle\phi^2\rangle V^2, \\ \langle\Delta v_y^2\rangle/\Delta t &= \tfrac{1}{2}\langle\phi^2\rangle V^2, \\ \langle\Delta v_z^2\rangle/\Delta t &= -\langle\phi^2\rangle V^2. \end{aligned} \tag{A11}$$

Transforming Eq. (A6) into spherical coordinates, using Eqs. (A9)–(A11), taking the limit $\Delta t \to 0$, and integrating over all angles ϕ, we obtain

$$\begin{aligned} &\partial P(V, \theta, t)/\partial t \\ &\quad = \tfrac{1}{2}\langle\phi^2\rangle(1/\sin\theta)(\partial/\partial\theta) \sin\theta(\partial P/\partial\theta). \end{aligned} \tag{A12}$$

The collision frequency is defined by

$$\langle\phi^2\rangle = Z\omega_p^4 \ln \Lambda^2/8\pi n V^3. \tag{A13}$$

Equation (A12) is identical to the Fokker–Planck collision term Q.E.D.